Recoil-distance lifetime measurements of ^{48}V levels*

B. A. Brown,† D. B. Fossan, J. M. McDonald,‡ and K. A. Snover§
Department of Physics, State University of New York, Stony Brook, New York 11794
(Received 9 December 1974)

Lifetimes for a number of levels in ^{48}V have been measured using the recoil-distance technique. The experimental results for the mean lifetimes are 8.8±1.4 psec for the 428-keV 5^+ level, 21.6±1.1 psec for the 613-keV 4^+ level, 111±9 psec for the 627-keV 6^+ level, 6.7±1.8 psec for the 1056-keV 3^- level, and 6.5±0.5 psec for the 1099-keV $4^{(-)}$ level. Lifetime limits were measured for other levels. The electromagnetic transition strengths for the positive and negative parity bands are discussed. For the positive parity levels, shell model calculations are carried out assuming wave functions of the form $(\pi f_{7/2})^n(\nu f_{7/2})^{-n}$. Many properties of ^{48}V and surrounding nuclei, particularly for the high-spin states, can be described using the ^{42}Sc effective interaction with effective operators $e_p+e_n=2$ and $g_p-g_n=1.29$. For some aspects, however, the effective operator approach within this limited $1f_{7/2}$ model space is not adequate.

[NUCLEAR REACTIONS ^{45}Sc(α,n) $E=9.5$ MeV; measured n-γ coin, deduced levels in ^{48}V; measured recoil distance, deduced $T_{1/2}$, $B(L)$, π assignments. Natural target, Ge(Li) detectors.]

I. INTRODUCTION

The simplest shell model configuration for the odd-odd nucleus ^{48}V is $(\pi f_{7/2})^3(\nu f_{7/2})^{-3}$. Within this configuration the electromagnetic matrix elements obey simple selection rules and are rather independent of the assumed residual two-body interaction.[1] For example, the calculated g factors for all levels are the same, $g=\frac{1}{2}(g_p+g_n)$. However, experimentally the g factors of the ground state and first excited state[2] differ by nearly a factor of 2, which suggests that admixtures from other $1f$-$2p$ orbitals are important. A knowledge of the electromagnetic properties of other positive parity levels is important for further tests of the theoretical model. Of additional interest are the properties of the recently discovered[3,4] low-lying negative parity rotational bands in ^{48}V. Previously, several experiments[3-7] have been carried out to determine the spins, branching ratios, and mixing ratios for a number of the excited levels. Only limited lifetime information[2,5,6] for states in ^{48}V existed. In the present experiment the recoil-distance (plunger) method has been used to measure mean lifetimes in the range 3 psec$<\tau<$500 psec for levels in ^{48}V below 2 MeV. This experiment was part of a series of plunger lifetime experiments which were carried out for $1f_{7/2}$ shell nuclei.[8]

The ^{48}V excited states were studied using singles γ-ray spectra from the ^{45}Sc$(\alpha,n)^{48}$V reaction. This reaction populates most strongly the series of yrast levels consisting of the lowest state of each spin and parity. The γ rays originating from ^{48}V were identified with a neutron-γ [Ge(Li)] coincidence experiment. In addition to ^{48}V, levels in ^{48}Ti were also strongly populated by the ^{45}Sc(α,p)-^{48}Ti reaction; the plunger lifetime results for ^{48}Ti have been reported previously.[8]

The decay scheme for ^{48}V based on previous experiments is shown in Fig. 1. Of most importance for the low-lying levels are the results of Samuelson *et al.*[4,5] using ^{48}Ti(p,n) and ^{46}Ti(α,pn); Huber *et al.*[6] using ^{40}Ca(^{10}B, $2p$) and ^{40}Ca(^{12}C, $3pn$); and Haas and Taras[3] using ^{34}S(^{16}O, pn). From these experiments, the parities have been definitely assigned only for the lowest 4^+, 2^+, 1^+, and 1^- levels, although spin assignments have been made for many other levels.

In Sec. II the recoil distance measurements[8-10] are reviewed briefly, while the lifetime results are discussed in Sec. III along with several parity assignments. In Sec. IV, the transition strengths for the positive and negative parity bands in ^{48}V are presented. Transition-strength comparisons for ^{48}V as well as for the neighboring nucleus ^{48}Ti are made with the shell model calculations. The energies of the positive parity levels in ^{48}V are also compared with shell model calculations using several effective interactions. Preliminary results for the present work have been reported previously.[11]

II. EXPERIMENTAL TECHNIQUE

The plunger apparatus used in the present experiment has been described previously.[9] The re-

action ^{45}Sc$(\alpha,n)^{48}$V with $E_\alpha = 9.5$ MeV was used. The target consisted of 70 μg/cm^2 scandium metal evaporated onto 3 mg/cm^2 Au backing foil. It was oriented with the Au foil facing the beam and positioned in the plunger apparatus by means of a V-groove O-ring arrangement designed to hold the target flat. The recoiling excited nuclei were kinematically confined to a forward cone with a half angle of 25°.

The excited nuclei, which recoil with a velocity component v in the direction of the beam and decay in flight, will emit γ rays at 0° to the beam with a shifted energy $E_s = E_0(1 + v/c)$. A flat Au plunger positioned at a distance $D - D_0$ from the target stops the recoiling nuclei so that those which decay at a time greater than the flight time $t = (D - D_0)/v$ will emit γ rays with an unshifted energy E_0. The γ-ray energy spectra were measured at 0° with a 45-cm^3 Ge(Li) detector which had a resolution of about 2.5 keV at 1332 keV. Because of the typically low energy of the measured γ rays, the stopped and shifted peaks were not well resolved; see for example Fig. 4. On the basis of previous experience with cases which were well resolved,[8] the corresponding peak areas I_0 and I_s were determined from the line shape by a simultaneous least-squares fit with Gaussian and skew-Gaussian shapes, respectively. The parameters for the skew-Gaussian shape were determined from a spectrum at a large distance $D - D_0 \gg v\tau$. The experimental ratios R of the unshifted area to the total area, $I_0/(I_0 + I_s)$, were then formed from the measurements at each distance.

The experimental ratios obtained as a function of D were fitted with the formula

$$R(D - D_0) = A \sum_i a_i e^{-(D-D_0)/v_i\tau} + R_\infty , \qquad (1)$$

where $A + R_\infty = 1$. The background ratio R_∞ is measured with a good statistical accuracy at a distance of $D - D_0 \gg v\tau$. The a_i represent the fraction ($\sum a_i = 1$) of nuclei recoiling with velocity v_i and are determined from the experimental shape of the shifted peak after unfolding the detector resolution. The lifetime values obtained using Eq. (1) differed only a few percent from the lifetimes determined from the first-order equation

$$R = Ae^{-(D-D_0)/\bar{v}\tau} + R_\infty , \qquad (2)$$

where $\bar{v}$ is the mean recoil velocity. In the present experiment typically $\bar{v}/c = 0.6\%$. The final values of τ were obtained after several small corrections were made. These include corrections for the finite solid angle of the detector, for efficiency

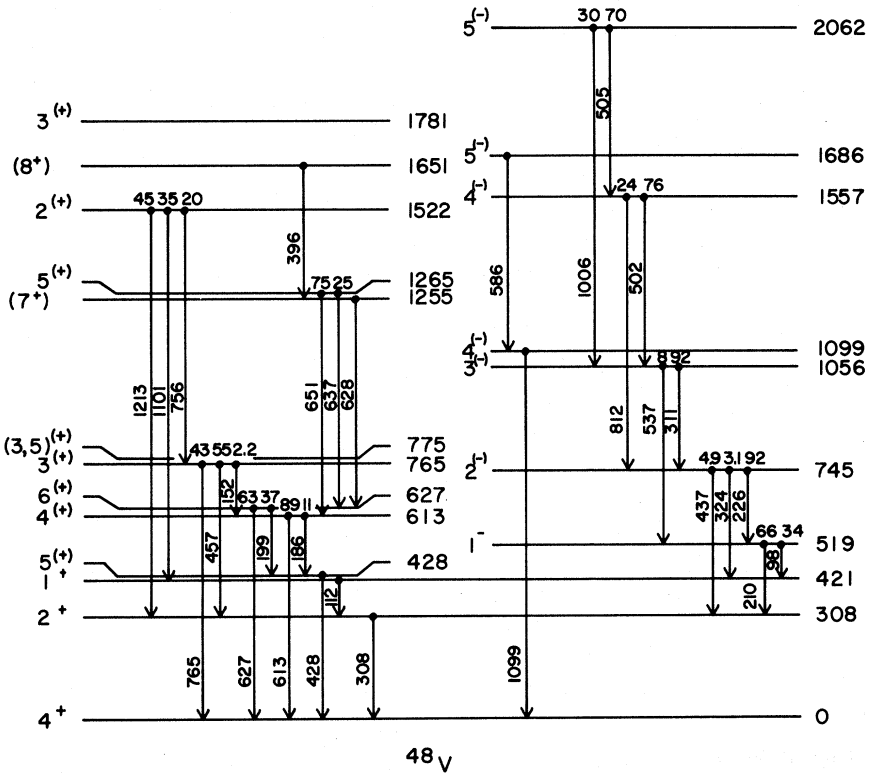

FIG. 1. The decay scheme for low lying ^{48}V levels. The data are summarized from Refs. 3–6.

TABLE I. Mean lifetimes of ^{48}V levels.

Energy (keV)	J^π	τ (psec) Present work	Other
308	2^+		$(10.26\pm0.06)\times10^3$ [a] $(10.1\pm0.1)\times10^3$ [b]
428	5^+	8.8 ± 1.4	≤ 20 [c]
519	1^-		$(3.92\pm0.09)\times10^3$ [a]
613	4^+	21.6 ± 1.1	
627	6^+	111 ± 9	130 ± 60 [c]
745	2^-	≤ 30 [d]	~25, [e] $4<\tau<42$ [c]
765	3^+	≤ 3.7	
1056	3^-	6.7 ± 1.8	~5 [e]
1099	$4^{(-)}$	6.5 ± 0.5	
1255	$(7)^+$		≤ 10 [c]
1265	5^+	≤ 2.8	
1522	2^+	≤ 4.4	
1557	4^-	≤ 4.1	
1686	$5^{(-)}$	≤ 4.4	

[a] Reference 5.
[b] Reference 2.
[c] Reference 6.
[d] 2σ lifetime limits.
[e] Reference 3.

variations of the peak areas I_0 and I_s, and for higher order relativistic effects.[9] Also, the quoted errors take into account the estimated effect of the hyperfine field deorientation.[8]

Since the lifetimes were determined from singles γ spectra, the question of feeding from higher levels must be considered, as the α bombarding energy is appreciably higher than the kinematical threshold for the production of the levels of interest. To insure that any feeding levels did not influence the measured decay curves, the lifetimes associated with all cascade γ rays that feed the levels of interest were examined in the plunger data. In most cases upper limits could be established for levels which cascade to those of interest with any appreciable intensity. In one case, for the lifetime of the 428-keV level, it was required to fit the ratio data with a combination of two lifetimes in which the lifetime of the feeding level was known; see Sec. III. This data was fitted with the two-level formula given in Ref. 8.

III. EXPERIMENTAL RESULTS

The present lifetime results are summarized in Table I. The results for five levels which are within the plunger lifetime range are discussed individually below. Lifetime limits were obtained for an additional six levels. The lifetimes of the 308- and 519-keV levels were outside the plunger lifetime range; these lifetimes have been measured by Samuelson *et al.*[5] with the electronic timing technique. For the 421- and 745-keV levels, the primary decay γ rays for these levels were too low in energy to distinguish the stopped and shifted peaks in the present (α, n) experiment. A

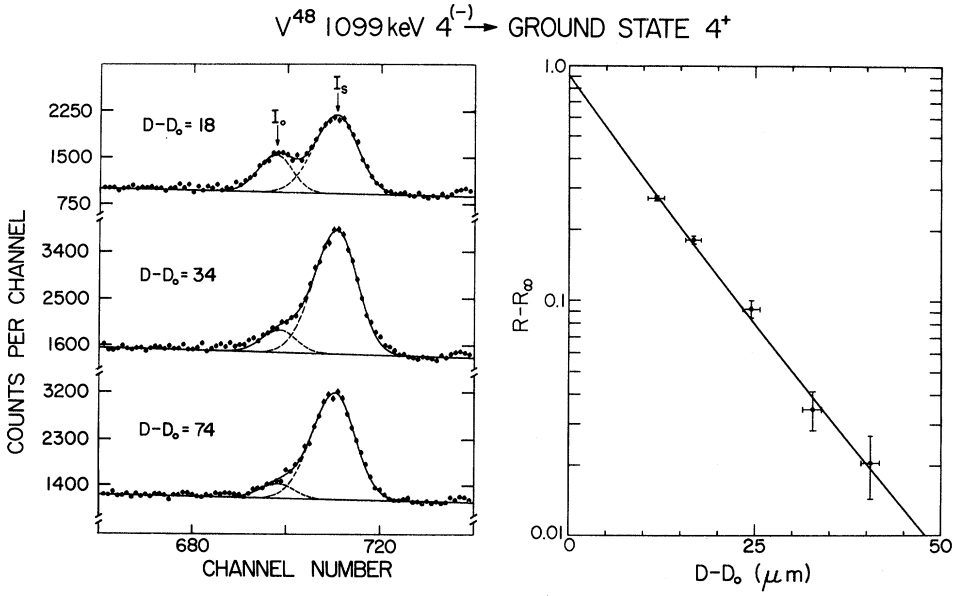

FIG. 2. Recoil-distance γ-ray spectra and lifetime decay curve for the 1099-keV→ ground-state transition. The left portion of the figure displays the γ-ray spectra in the region of the 1099-keV transition measured at three different plunger distances $D-D_0$ (in μm), with I_0 and I_s indicating the stopped and shifted peaks, respectively. The methods of extracting the I_0 and I_s areas are discussed in the text. The right portion of the figure is a semilogarithmic plot of $R-R_\infty$ vs $D-D_0$, where $R=I_0/(I_0+I_s)$. The curve through the ratio data represents a least-squares fit of Eq. (1) to the data as described in the text.

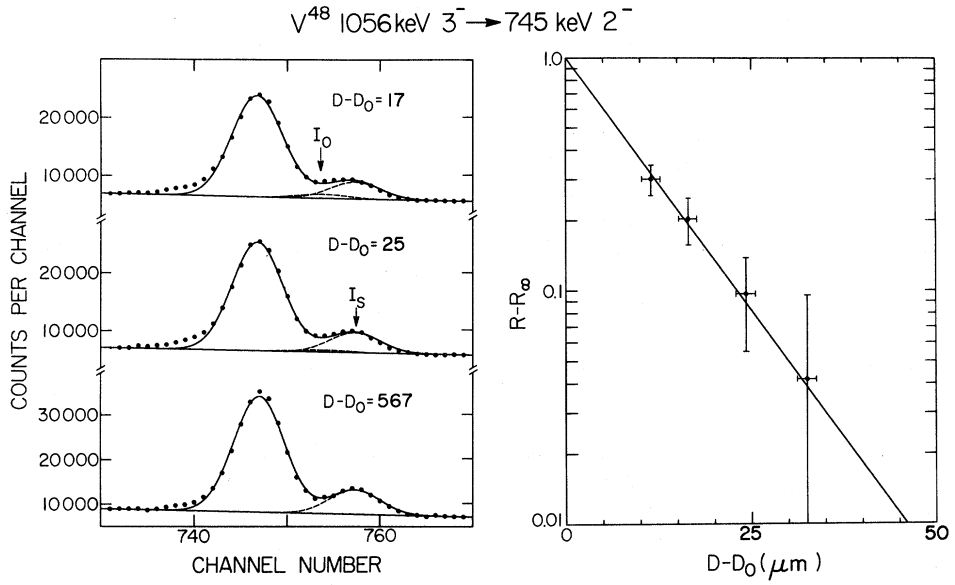

FIG. 3. Recoil-distance γ-ray spectra and lifetime decay curve for the 1056-keV→745-keV transition. The presentation is similar to that of Fig. 2. The line shape consists of three peaks: I_0(308 keV), I_0(311 keV), and I_s(311 keV) (see text).

lifetime limit was obtained for the 745-keV level from the weak 437-keV γ branch. The lifetimes of these two levels would be measurable by the recoil distance method (RDM) using a heavy ion reaction to achieve a larger recoil velocity.

1099 keV

The lifetime of the 1099-keV level was measured using the 1099-keV decay γ ray to the ground state. The γ spectra at three typical plunger distances are shown on the left in Fig. 2. The individual contributions from the areas I_0 and I_s for the stopped and shifted peak, respectively, are indicated with dashed lines. On the right in this figure the ratio data, $R - R_\infty$, are shown together with the fit using Eq. (1). The fit gave a mean lifetime of $\tau = 6.5 \pm 0.5$ psec for the 1099-keV level. This level is weakly fed from the 1686-keV level for which a

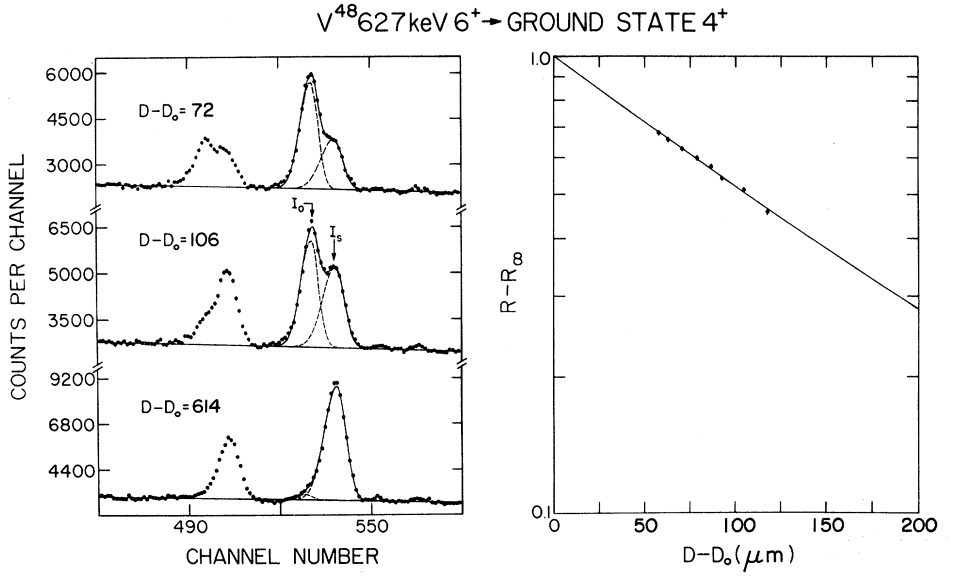

FIG. 4. Recoil-distance γ-ray spectra and lifetime decay curve for the 627-keV→ ground state transition. The presentation is similar to that of Fig. 2.

mean lifetime upper limit (2σ) of 4.4 psec was determined.

1056 keV

The 1056-keV → 745-keV transition was used to measure the lifetime of the 1056-keV level. The analysis of this 311-keV transition was complicated by the strong 308-keV $2^+ \rightarrow 4^+$ transition which is unshifted due to its long lifetime. The spectra, see Fig. 3, were fitted simultaneously with three peaks; $I_0(308)$, $I_0(311)$, and $I_s(311)$. The separation energy $E_0(311) - E_0(308) = 2.5$ keV was fixed by using the energies given by Samuelson *et al.*[5] and $E_s(311) - E_0(308)$ was determined from a spectra taken at a large plunger distance $D - D_0 \gg \bar{v}\tau$. The ratio data, shown on the right of Fig. 3, yielded a mean lifetime $\tau = 6.7 \pm 1.8$ psec for the 1056-keV level. This level is weakly fed by the 1557-keV level for which an upper limit (2σ) of 4.1 psec was obtained for the mean lifetime.

627 keV

The 627-keV → ground-state γ ray was used to measure the lifetime of this level. Typical γ-ray spectra and the decay curve are shown in Fig. 4. The result for the mean lifetime is $\tau = 111 \pm 9$ psec. In the present work this lifetime can be attributed to either the 627- or 1255-keV levels due to the unresolved γ cascade 628- and 627-keV. However, when compared with previous results of $\tau = 130 \pm 60$ psec for the 627-keV level and $\tau \leq 10$ psec for the 1255-keV level,[6] the present result must be attributed to the lifetime of the 627-keV level.

The 627-keV level is also weakly fed indirectly from the 1651-keV level and directly from the 1265-keV level ($\tau \leq 2.8$ psec) which do not affect the $\tau = 111 \pm 9$ psec result.

613 keV

The lifetime of the 613-keV level was measured via the 613-keV → ground-state transition. Typical γ-ray spectra and the decay curve are shown in Fig. 5. The measured mean lifetime is $\tau = 21.6 \pm 1.1$ psec for the 613-keV level. Short lifetime limits were obtained for all cascade transitions to this level.

428 keV

The 428-keV → ground-state transition was used to measure the lifetime of this level. Typical γ-ray spectra and the decay curve are shown in Fig. 6. The decay curve is clearly composed of at least two lifetimes. The strongest feeding originates from the 627-keV ($\tau = 111 \pm 9$ psec) → 428-keV transition. There is also weaker feeding from the 613-keV ($\tau = 21.6 \pm 1.1$ psec) level. From the relative intensities of the γ rays in the present experiment and branching ratios given by Samuelson *et al.*,[5] the indirect feeding fractions[8] to the 428-keV level are $f'(627) = 24\%$ and $f'(613) = 2.6\%$. The feeding from the 613-keV level can be neglected. The decay curve was fitted with a sum of two exponentials [Eq. (4) of Ref. 8] in which the feeding lifetime $\tau = 111 \pm 9$ psec was fixed. The result for the 428-keV mean lifetime is $\tau = 8.8 \pm 1.4$ psec. The fit to the decay curve in Fig. 6 is decomposed

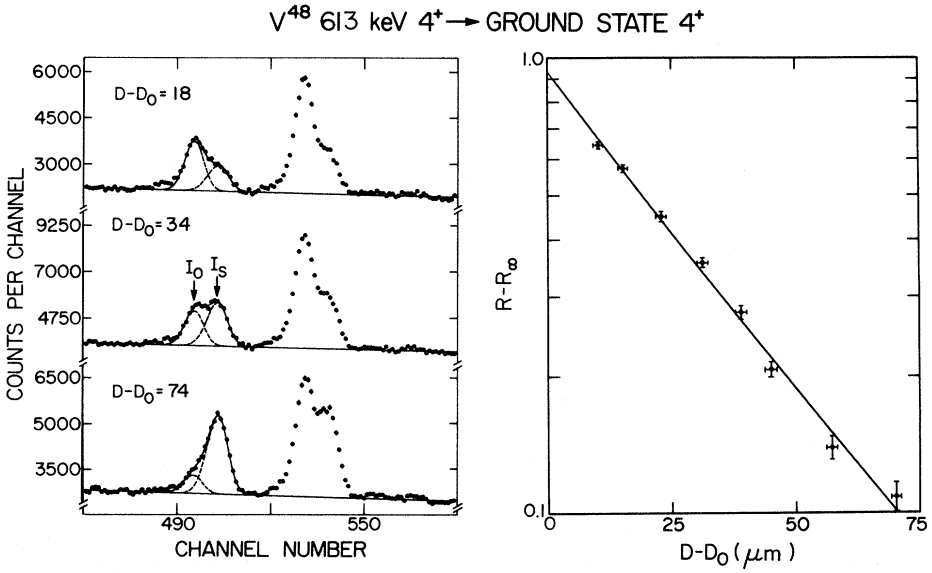

FIG. 5. Recoil-distance γ-ray spectra and lifetime decay curve for the 613-keV → ground-state transition. The presentation is similar to that of Fig. 2.

to show the separate contribution from the short and long lifetime components.

Parity assignments

The transition strengths from the present measurements can be used to obtain the parities of a number of levels whose spins have been determined previously. The observed transitions in ^{48}V can be classified into two main bands (see Fig. 1), those which decay through the 519-keV 1^- level shown on the right in Fig. 1, and those on the left which do not. Also, another band is believed to start from the 1099-keV $4^{(-)}$ level.[4]

The transition strengths for the 1056-keV $J=3 \rightarrow$ 519-keV 1^- transition are 22 Weisskopf units (W.u.) for $E2$, 9×10^2 W.u. for $M2$, and 12×10^6 W.u. for $E3$. Only the $E2$ is reasonable, which implies a negative parity assignment for the 1056-keV level. In a similar manner the transition strengths for other transitions within this band give negative parity assignments to the 745- and 1557-keV levels. This is supported by previous tentative negative parity assignments for these levels.[3,4]

The transition strengths for the levels which eventually decay to the 2^+ 308-keV level or 4^+ ground state suggest positive parity for the 428-, 613-, 627-, 765-, 1255-, 1265-, and 1522-keV levels. The transition strengths for the 1099-keV $J=4 \rightarrow$ ground state 4^+ transition of 8.6×10^{-5} W.u. for $E1$ and 7.6 W.u. for $E2$ support either parity assignment based on the observed strengths for other $E1$ and $E2$ transitions in this nucleus; see Tables II and III. Previously the 1099-keV level had been tentatively assigned a negative parity.[4]

IV. DISCUSSION AND COMPARISON WITH THEORY

Negative parity levels

The reduced transition probabilities for the ^{48}V transitions involving negative parity states and those between positive parity levels are summarized in Table II and Table III, respectively. The $E1$ transitions are hindered by factors of between 10^4 and 10^5 relative to the Weisskopf estimate. Also, the $E2$ transitions involving the negative parity levels are enhanced both relative to the Weisskopf estimate and relative to $E2$ transitions between the positive parity levels. These properties are consistent with the properties of other unlike parity rotational bands found in this mass region which involve $(sd)^{-1}(fp)^{n+1}$ configurations.[12,13]

In ^{48}V the Nilsson orbits[14] expected to participate in the negative parity levels are $[\pi 202\downarrow \frac{3}{2}^+]$ and $[\nu 312\uparrow \frac{5}{2}^-]$ for a prolate deformation (specified by the asymptotic quantum numbers $Nn_3\Lambda\Sigma$ and Ω^π). A total angular momentum along the symmetry axis of $K=1^-$ or 4^- is possible for these orbits. The coupling rules of Gallagher and Moszkowski[15] correctly predict the lowest to be $K=1^-$ and the most probable candidate for the $K=4^-$ state is the observed $J=4$ level at 1099 keV. Low-lying $\frac{3}{2}^+$

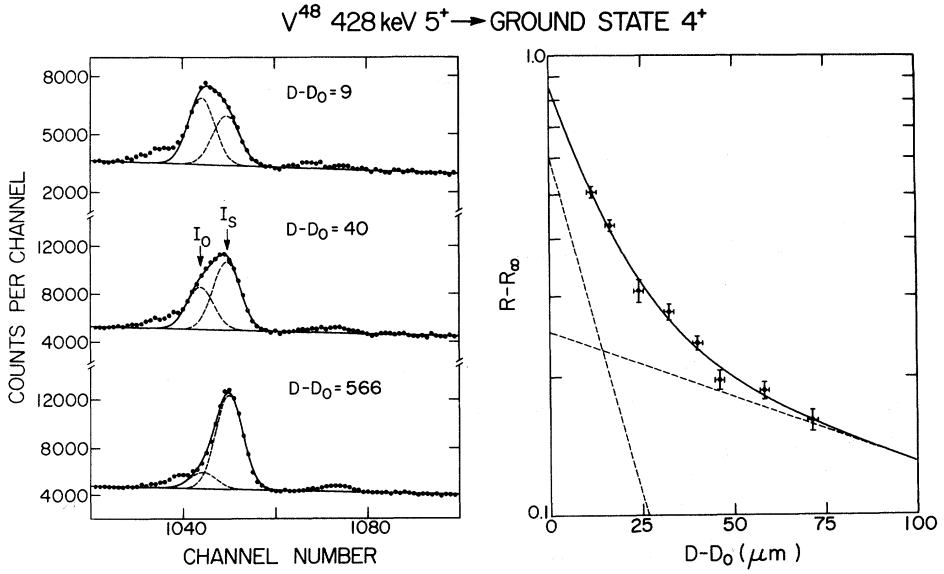

FIG. 6. Recoil-distance γ-ray spectra and lifetime decay curve for the 428-keV → ground-state transition. The presentation is similar to that of Fig. 2 except that the ratio data was fitted with a sum of two exponentials [Eq. (4) in Ref. 8] to take into account feeding from the 627-keV level. The dashed lines indicate the separate contributions from the long and short lifetime components.

TABLE II. Electromagnetic properties of ^{48}V involving negative parity levels.

E_i (keV)	τ [a] (psec)	$E_f(E_\gamma)$ [b] (keV)	$J_i \to J_f$	Branching [c] ratio (%)	Mixing ratio	$B(E1)$ [d] (W.u.$\times 10^{-5}$)	$B(M1)$ [d] (W.u.)
519	$(3.92\pm0.09)\times10^3$	308(210.4)	$1^- \to 2^+$	66 ± 5		1.34 ± 0.11	
		421(98.0)	$1^- \to 1^+$	34 ± 5		6.8 ± 1.1	
745	~ 25	308(324.2)	$2^- \to 2^+$	3.1 ± 0.3		~ 2.7	
		421(436.8)	$2^- \to 1^+$	4.9 ± 0.4		~ 1.8	
1099	6.5 ± 0.5	0(1099.3)	$4^{(-)} \to 4^+$	100		8.6 ± 0.7	
						$B(E2)$ [d] (W.u.)	
745	~ 25	519(226.3)	$2^- \to 1^-$	92 ± 1	0.06 ± 0.01 [c]	~ 17	~ 0.10
1056	6.7 ± 1.8	519(537.2)	$3^- \to 1^-$	8.5 ± 2	$E2$	22 ± 7	
		745(310.8)	$3^- \to 2^-$	91.5 ± 2	$-0.02\le\delta\le0.07$ [e]	≤ 25	0.145 ± 0.045
1557	≤ 4.1	745(812.2)	$4^- \to 2^-$	24 ± 3	$E2$	≥ 10	
		1056(501.8)	$4^- \to 3^-$	76 ± 3	0.12 ± 0.04 [e,f]	≥ 3	≥ 0.04
1686	≤ 4.4	1099(586.3)	$5^{(-)} \to 4^-$	100	$(M1)$		≥ 0.03

[a] From Table I.
[b] Reference 5.
[c] Average from Refs. 3 and 5.
[d] The definition of Weisskopf unit (W.u.) follows that of Wilkinson in *Nuclear Spectroscopy*, edited by F. Ajzenberg-Selove (Academic, New York, 1960), Part B, pp. 859–860; W.u. $(E1)=0.851\,e^2\mathrm{fm}^2$, W.u. $(E2)=10.36\,e^2\mathrm{fm}^4$, and W.u. $(M1)=1.79\mu_N{}^2$.
[e] Reference 3.
[f] Samuelson *et al.* (Ref. 5) give $-0.11\le\delta\le0.06$ for this transition.

levels which are related to $[\pi 2p\tfrac{3}{2}^+]$ orbits have also been observed in neighboring odd-even nuclei, ^{47}V (262 keV) and ^{49}V (748 keV).[16] Also in ^{46}Sc the 1^- state has been observed at 143 keV and a possible 4^- state at 627 keV.[16]

In the Nilsson model, the $E2$ matrix elements are complicated by the dependence, for $K=1$, on two intrinsic matrix elements $\langle K|T^{(2)}_0|K\rangle$ and $\langle K|T^{(2)}_{-2}|-K\rangle$.[14] For an axially symmetric shape the second intrinsic matrix element does not contribute in which case, for the $3^- \to 1^-$ transition, $Q_0 = |\langle K|T^{(2)}_0|K\rangle| = 116\pm20$ fm^2. If a very simple rigid body model is assumed, this value of Q_0 implies $\hbar^2/2\mathcal{I}_{\mathrm{rig}} \approx 50$ keV which is near to the value $\hbar^2/2\mathcal{I} = 56.7$ keV obtained[3] from the $J(J+1)$ spacing of the energy levels. This rotational-band description can describe the $2^- \to 1^-$ and $3^- \to 2^-$ $M1$ transitions using a reasonable value of $g_R - g_\Omega = 1.6\mu_N$.

TABLE III. Electromagnetic properties of ^{48}V involving transitions between positive parity levels.

E_i (keV)	τ [a] (psec)	$E_f(E_\gamma)$ [b] (keV)	$J_i \to J_f$	Branching [b] ratio (%)	Mixing [b] ratio	$B(E2)$ (e^2fm^4)	$B(M1)$ ($\mu_N{}^2\times10^{-2}$)
308	$(10.27\pm0.06)\times10^3$	0(308.3)	$2^+ \to 4^+$	100	$E2$	28.5 ± 0.2	
428	8.8 ± 1.4	0(427.9)	$5^+ \to 4^+$	100	$-0.15\le\delta\le-0.12$	120 ± 45	8.1 ± 1.3
613	21.6 ± 1.1	0(613.4)	$4^+ \to 4^+$	89 ± 2	$-0.21\le\delta\le-0.17$	13.7 ± 3.5	0.98 ± 0.06
		428(185.5)	$4^+ \to 5^+$	11 ± 2	$-0.02\le\delta\le+0.07$	≤ 110	4.5 ± 0.9
627	111 ± 9	0(627.3)	$6^+ \to 4^+$	63 ± 5	$E2$	48 ± 5	
		428(199.3)	$6^+ \to 5^+$	37 ± 5	$-0.28\le\delta\le+0.03$	≤ 510	2.3 ± 0.4
765	≤ 3.7	0(764.9)	$3^+ \to 4^+$	43 ± 2	$-0.05\le\delta\le0.00$		≥ 1.4
		308(456.7)	$3^+ \to 2^+$	55 ± 2	$-0.03\le\delta\le-0.01$	≥ 0.6	≥ 8.5
		613(151.7)	$3^+ \to 4^+$	2.2 ± 0.3	$(M1)$		≥ 8.4
1255	≤ 10	627(628)	$(7^+) \to 6^+$	100	$(M1)$		≥ 2.3
1265	≤ 2.8	613(651.2)	$5^+ \to 4^+$	75 ± 4	$-0.26\le\delta\le-0.03$	≥ 1.6	≥ 4.9
		627(637.3)	$5^+ \to 6^+$	25 ± 4	$(M1)$		≥ 1.6
1522	≤ 4.4	308(1212.9)	$2^+ \to 2^+$	45 ± 4	$+0.14\le\delta\le+0.28$	≥ 0.6	≥ 0.3
		421(1101.0)	$2^+ \to 1^+$	35 ± 4	$-0.05\le\delta\le+0.03$		≥ 0.3
		765(756.4)	$2^+ \to 3^+$	20 ± 2	$-0.02\le\delta\le+0.13$		≥ 0.5

[a] From Table I.
[b] Reference 5.

TABLE IV. Properties of electromagnetic matrix elements using $(\pi j)^n(\nu j)^m$ wave functions where $m=n$ or $m=-n$.

	Signature change	$M1$ transition [a]	$E2$ transition	g factor [a]	Q moment
$m=-n$	+	forbidden	$\sim(e_p-e_n)$	$=\frac{1}{2}(g_p+g_n)$	$\sim(e_p-e_n)$
	−	$\sim(g_p-g_n)$	$\sim(e_p+e_n)$		
$m=n$	+	forbidden	$\sim(e_p+e_n)$	$=\frac{1}{2}(g_p+g_n)$	$\sim(e_p+e_n)$
	−	$\sim(g_p-g_n)$	$\sim(e_p-e_n)$		

[a] $g=g_l\pm\dfrac{(g_s-g_l)}{2l+1}$ for $j=l\pm\frac{1}{2}$.

However, $M1$ transitions involving these core excited states in other nuclei in this region, for example ^{43}Sc,[12] ^{44}Sc,[13] and ^{45}Sc,[12] are hindered by a factor of 10–100 compared to the present results in ^{48}V.

Positive parity levels

In the shell model the simplest configuration which can be assumed for the positive parity states in ^{48}V is $(\pi f_{7/2})^3(\nu f_{7/2})^{-3}$. It is interesting to try to explain the properties of this self-conjugate nucleus in the middle of the $1f_{7/2}$ shell with these simple wave functions using effective operators. The effective operators would take into account small admixtures of other configurations including those involving other $1f$-$2p$ orbitals. This approach using $(f_{7/2})^n$ wave functions has proved rather successful in describing both energy levels[17] and electromagnetic transition strengths[8] for the low lying levels in the isotones with 28 neutrons. However, at the beginning of the $1f_{7/2}$ shell it is well known that many properties cannot be described with such simple wave functions.[8]

Wave functions of the type $(\pi f_{7/2})^n(\nu f_{7/2})^m$ where $m=n$ or $m=-n$ can be classified according to their transformation properties under the exchange of protons and neutrons.[1] The signature[1] of the wave functions

$$\psi_M^J=\sum_{J_1J_2}\alpha_{J_1J_2}[(\pi f_{7/2})^n J_1\otimes(\nu f_{7/2})^m J_2]_M^J\ ,$$

where $m=n$ or $m=-n$ is defined by the $\pm$ sign in the expression $\alpha_{J_1J_2}=\pm(-1)^{J_1+J_2-J}\alpha_{J_2J_1}$. As a result of this symmetry property the electromagnetic matrix elements are proportional to either the sum or the difference of the effective proton and neutron operators. These properties are summarized in Table IV. In the case $m=n$ the signature change is simply the change in isospin $(-1)^{\Delta T}$ and the selection rules are the well known isospin selection rules.

In the present case of interest where $m=-n$, the change from particle to hole can be obtained from the particle-hole transformation of a tensor of rank k: $\langle j^{-n}\|T^k\|j^{-n}\rangle=(-1)^{k+1}\langle j^n\|T^k\|j^n\rangle$. Although the signature cannot be related to any simple quantity such as the isospin in this case, certain selection rules do exist. $M1$ transitions are

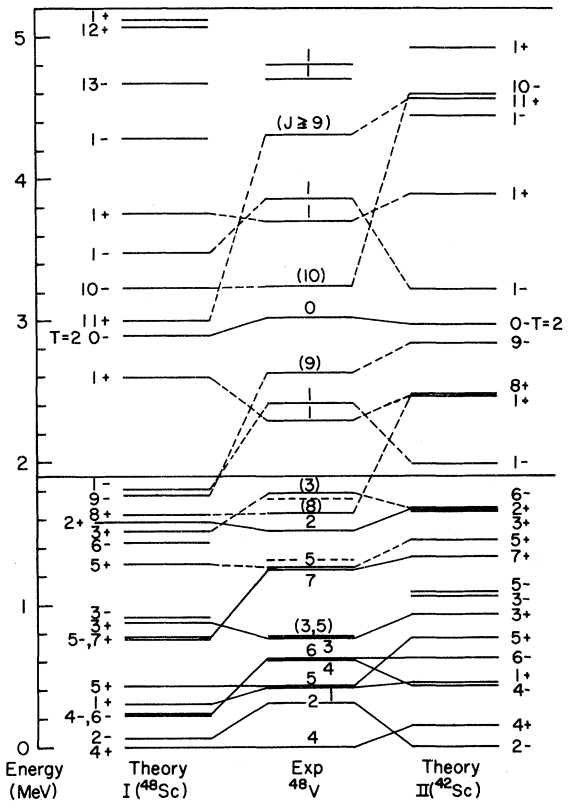

FIG. 7. Comparison of calculated and experimental positive parity levels in ^{48}V. The levels have been calculated assuming two effective two-body interactions: (I) using the Pandya transformation of the ^{48}Sc spectrum and (II) using the ^{42}Sc spectrum. The calculated levels are labeled by the spin and signature (see text). Below 1.9 MeV all levels are shown, above 1.9 MeV only the yrast and $J=0$ and 1 levels are shown. The experimental levels not shown in Fig. 1 are from Ref. 19 (dashed lines), Ref. 7 for $J=0$ and 1, and Ref. 25 for the high-spin levels.

TABLE V. Comparison of calculated and experimental electromagnetic matrix elements for positive parity levels in ^{48}V and ^{48}Ti. Two effective two-body interactions are assumed; (I) using the Pandya transformation of the ^{48}Sc spectrum and (II) using the ^{42}Sc spectrum.

Nucleus	$J_i \to J_f$	Signature change	$B(E2)_{exp}$ (e^2 fm^4)	$B(E2)_{th}$ (e^2 fm^4) [a] I(^{48}Sc)	$B(E2)_{th}$ (e^2 fm^4) [a] II(^{42}Sc)	$B(M1)_{exp}$ ($\mu_N^2 \times 10^{-2}$)	$B(M1)_{th}$ ($\mu_N^2 \times 10^{-2}$) [b] I(^{48}Sc)	$B(M1)_{th}$ ($\mu_N^2 \times 10^{-2}$) [b] II(^{42}Sc)
^{48}V	$2_1 \to 4_1$	−	28.5 ± 0.2	95.3	92.2			
	$1_1 \to 2_1$	−		115	103		233	227
	$5_1 \to 4_1$	+	120 ± 45	0.79	0.75	8.1 ± 1.3	0	0
	$4_2 \to 4_1$	−	13.7 ± 3.5	86.6	81.9	0.98 ± 0.06	0.55	0.88
	$4_2 \to 5_1$	−	≤110	107	99	4.5 ± 0.9	28.4	39.9
	$6_1 \to 4_1$	−	48 ± 5	47.8	49.0			
	$6_1 \to 5_1$	−	≤510	67.0	56.3	2.3 ± 0.4	0.57	3.06
	$3_1 \to 4_1$	+		1.70	1.99	≥1.4	0	0
	$3_1 \to 2_1$	−	≥0.6	57.2	60.2	≥8.5	174	113
	$3_1 \to 4_2$	−		14.1	12.0	≥8.4	0.0	0.52
^{48}Ti	$2_1 \to 0_1$	−	140 ± 5 [c]	52.1	51.1			
	$2_2 \to 0_1$	+	13.9 ± 3.4 [d]	5.94	6.57			
	$2_2 \to 2_1$	−	63^{+100}_{-50} [d]	48.4	44.0	50 ± 11 [d]	53.6	55.6
	$4_1 \to 2_1$	−	88 ± 26 [d]	64.7	63.8			
	$4_2 \to 2_1$	+	≤0.5 [d]	2.75	3.28			
	$4_2 \to 4_1$	−		0.89	0.31	143 ± 60 [d]	130	117
	$3_1 \to 2_1$	+	16^{+6}_{-9} [d]	8.38	8.94	7.7 ± 2.9 [d]	0	0
	$3_1 \to 4_1$	−		27.9	26.6	43 ± 16 [d]	28.0	28.3
	$3_1 \to 2_2$	−		72.7	69.1	9.5 ± 3.6 [d]	11.0	8.69
	$6_1 \to 4_1$	−	53 ± 5 [e]	46.6	47.1			

[a] Effective charges of $e_p + e_n = 2$ and $e_p - e_n = 1$ for negative and positive signature change, respectively, have been used. The r^2 radial matrix elements were calculated with $\hbar\omega = 41A^{-1/3}$ MeV.

[b] $g_p - g_n = 1.29$.

[c] Average from Refs. 21–23.

[d] Reference 24.

[e] Reference 8.

forbidden for no-signature-change transitions. In addition, the $B(E2)$ values for transitions with no signature change are typically an order of magnitude less than those involved in a signature change; only part of this reduction is due to the factor $(e_p - e_n)^2/(e_p + e_n)^2 \approx \frac{1}{4}$. Thus in all cases the transitions which do not change the signature are theoretically hindered and many aspects of the decay scheme can be predicted without detailed calculations of the one-body matrix elements.

The positive parity levels have been calculated with two sets of effective two-body interactions, (I) using the Pandya transformation of ^{48}Sc energy levels and (II) using ^{42}Sc energy levels.[18] For $J = 0$ through 7, these two-body matrix elements are (I) 0, 11, 1310, 1082, 2188, 1261, 2402, and −148 keV, and (II) 0, 611, 1586, 1491, 2817, 1511, 3237, and 618 keV.

The calculated and experimental energy levels are compared in Fig. 7. Most of the experimental levels shown in the figure have been well established by their γ decay, but below 1.9 MeV two additional levels which have been observed in an ^{50}Cr$(d, \alpha)^{48}$V experiment[19] have been included (indicated by dashed lines). The experimental and calculated levels have been shifted to a common ground-state energy for comparison purposes. In this way the calculated $T = 2, 0^+$ ground-state analog of ^{48}Ti is in good agreement with experiment. The difference between the calculated and the experimental binding energy of ^{48}V is 1.89 MeV with interaction I(^{48}Sc) and 0.38 MeV with interaction II(^{42}Sc), using the ^{43}Ti-^{43}Sc Coulomb energy shift of 10.85 MeV.

The first six levels are easily accounted for by the calculation; however, the correct ground-state spin is predicted only by the I(^{48}Sc) interaction. Beyond the first six levels the correspondence between experiment and theory is more ambiguous. In some cases, an association between experiment and theory has been made on the basis of the observed decay modes. For example the 1265-keV $J = 5$ level which is observed to decay to the 613-keV $J = 4$ and 627-keV $J = 6$ levels but not to the 428-keV $J = 5$ level is consistent with the predicted decay mode of the calculated third $J = 5$ level. The calculated second $J = 3$, 5, and 6 levels may correspond to three experimental levels in this region whose spins have not been assigned. The predicted decay modes are $3_2 \to 4_1$, $5_2 \to 4_1$, and $6_2 \to 5_1$.

As has been discussed previously,[7] the calculation does not predict the correct ordering of the pairs of $J=1$ levels above 1.9 MeV.

It is interesting to compare the yrast levels $J=4$–15 for which the predicted energy spread $\Delta E = E(J=15) - E(J=4)$ is quite different for the two effective interactions. They are $\Delta E = 6.54$ and 9.49 MeV for interactions I(^{48}Sc) and II(^{42}Sc), respectively. For these high spin states, except $J=8$ and 10, the results using the ^{42}Sc interaction are in much better agreement with experiment. The experimental results for $J \geq 8$ should be confirmed. Also, for other nuclei near ^{48}Sc such as ^{48}Ti and ^{49}Ti, the experimental yrast levels are predicted much better by the ^{42}Sc rather than the ^{48}Sc interaction. In ^{48}V the decay of the high-spin states is predicted to form two distinct bands $15 \rightarrow 13 \rightarrow 11 \rightarrow 9 \rightarrow 7$ and $14 \rightarrow 12 \rightarrow 10 \rightarrow 8 \rightarrow 6$ where crossover transitions of the type $15 \rightarrow 14$ are allowed but those of the type $14 \rightarrow 13$ are very hindered.

A quantitative comparison of the experimental and calculated electromagnetic matrix elements for the first seven positive parity levels in ^{48}V is given in Table V. The comparison is also made for transitions in the self-conjugate nucleus ^{48}Ti, $(\pi f_{7/2})^2 (\nu f_{7/2})^{-2}$, in which the calculated matrix elements are governed in the same way by the signature change. The matrix elements which are calculated to be relatively strong are rather insensitive to the assumed effective two-body interactions, whereas those that are relatively weak are more sensitive to the interaction and are also probably more sensitive to small admixtures of configurations outside the $(f_{7/2})^n$ model space.

For $E2$ transitions, effective charges of $e_p + e_n = 2$ and $e_p - e_n = 1$ have been used for the calculated matrix elements. The comparisons for the high-spin $6 \rightarrow 4$ transitions in both ^{48}V and ^{48}Ti are very good. However, other $E2$ transitions cannot be satisfactorily explained by this simple $(f_{7/2})^n$ model. Particularly interesting is the experimental hindrance of about a factor of 4 for the ^{48}V $2_1 \rightarrow 4_1$ and $4_2 \rightarrow 4_1$ transitions, which suggests that other configurations are important for these 2_1 and 4_2 states. The experimental g factors[2] of 0.41 for the 4_1 level and 0.188 for the 2_1 level compared to the calculated value of $g = 0.554$ for both levels also indicate a difference in the structure of the 2_1 level.

It may be possible to describe the ^{48}V positive parity levels in the deformed Nilsson scheme.[14] In this case the coupling rules of Gallagher and Moszkowski[15] correctly predict the ground state $K=4$ from the prolate configuration $[\pi 321 \uparrow \frac{3}{2}^-]$ plus $[\nu 312 \downarrow \frac{5}{2}^-]$. The excited $J=2_1$ state can be formed in several ways[2]; in one way, $[\pi 330 \uparrow \frac{1}{2}^-]$ plus $[\nu 321 \downarrow \frac{3}{2}^-]$, the $2_1 \rightarrow 4_1$ $E2$ transition is forbidden since the 2_1 and 4_1 states differ by a change of two particles. Detailed calculations of this type have not been carried out. In this scheme, band mixing[20] would be important since the positive parity level structure does not indicate any clear $J(J+1)$ energy dependence.

The $M1$ matrix elements have been calculated using an effective operator $g_p - g_n = 1.29$ which is reduced from the Schmidt value $g_p - g_n = 2.20$. This value gives good agreement with six experimental transitions in ^{48}V and ^{48}Ti. In ^{48}V, the calculated matrix elements using interaction II(^{42}Sc) are in better agreement with experiment than those using interaction I(^{48}Sc). However, also in ^{48}V several calculated $M1$ transitions are in very poor agreement with the experiment. The only measured transition which is predicted to be strong, $4_2 \rightarrow 5_1$, is hindered by about a factor of 10 from the calculated values. Also, one of the stronger observed $M1$ transitions, $5_1 \rightarrow 4_1$, is predicted to be forbidden.

In conclusion, some properties of ^{48}V and other neighboring nuclei can be quite well explained within an $(f_{7/2})^n$ model space, particularly regarding the yrast levels. In this respect the results obtained with an effective two-body interaction based on the ^{42}Sc spectrum is in better agreement than the results based on the ^{48}Sc spectrum. However, this model space is too limited to account for many of the observed properties especially for levels outside the yrast bands. Due to the abundance of experimental data in this mass region, enlarged shell-model calculations including other $1f$-$2p$ configurations would be interesting although not necessarily more illuminating because of the complexity of the spherical wave functions in this mass region.

ACKNOWLEDGMENTS

The authors would like to thank Dr. R. D. Lawson for helpful theoretical discussions and for providing ^{48}V wave functions. We also thank Dr. K. Ogawa for the use of his shell-model computer program.

*Work supported in part by the National Science Foundation.

†Present address: University of Tokyo, Tokyo, Japan.
‡Present address: Sloan-Kettering Institute, New York, New York.
§Present address: Physics Department, University of Washington, Seattle, Washington.

[1]R. D. Lawson, Nucl. Phys. A173, 17 (1971).
[2]K. Auerbach, J. Braunsfurth, M. Maier, E. Bodenstedt, and H. W. Flender, Nucl. Phys. A94, 427 (1967).
[3]B. Haas and P. Taras, Phys. Rev. Lett. 33, 105 (1974).
[4]L. E. Samuelson, F. M. Bernthal, W. H. Kelley, and Wm. C. McHarris, Bull. Am. Phys. Soc. 19, 546 (1974).
[5]L. E. Samuelson, W. H. Kelly, R. A. Warner, Wm. C. McHarris, E. M. Bernstein, and R. Shamu, in *Proceedings of the International Conference on Nuclear Physics, Munich, 1973,* edited by J. de Boer and H. J. Mang (North-Holland, Amsterdam/American Elsevier, New York, 1973), Vol. 1, p. 209; and private communication.
[6]R. B. Huber, C. Signorini, W. Kutschera, and H. Morinaga, Nuovo Cimento 15A, 501 (1973).
[7]J. W. Smith, L. Meyer-Schutzmeister, and G. Hardie, Phys. Rev. C 8, 2232 (1973).
[8]B. A. Brown, D. B. Fossan, J. M. McDonald, and K. A. Snover, Phys. Rev. C 9, 1033 (1974).
[9]K. W. Jones, A. Z. Schwarzschild, E. K. Warburton, and D. B. Fossan, Phys. Rev. 178, 1773 (1969).
[10]D. B. Fossan and E. K. Warburton, in *Nuclear Spectroscopy II,* edited by J. Cerny (Academic, New York, 1974), Chap. VII H, p. 307.
[11]B. A. Brown, J. M. McDonald, K. A. Snover, and D. B. Fossan, Bull. Am. Phys. Soc. 17, 933 (1972); J. M. McDonald, B. A. Brown, K. A. Snover, D. B. Fossan, and I. Plesser, Bull. Am. Phys. Soc. 16, 1183 (1971).
[12]P. R. Maurenzig, in *Proceedings of the Topical Conference on the Structure of $1f_{7/2}$ Nuclei, Padua, Italy, 1971,* edited by R. A. Ricci (Editrice Compositori, Bologna, 1971), p. 469.
[13]G. D. Dracoulis, J. L. Durell, and W. Gelletly, J. Phys. A6, 1030 (1973).
[14]S. G. Nilsson, K. Dan. Vidensk. Selsk. Mat. Fys.—Medd. 29, No. 16 (1955).
[15]C. J. Gallagher and S. A. Moszkowski, Phys. Rev. 111, 1282 (1958).
[16]Nuclear Data Group, *Nuclear Level Schemes $A = 45$ through $A = 257$,* edited by D. J. Horen (Academic, New York, 1973), p. $A = 47$, $A = 49$.
[17]A. R. Poletti, B. A. Brown, D. B. Fossan, and E. K. Warburton, Phys. Rev. C 10, 2312 (1974).
[18]J. P. Schiffer, in *Proceedings of the Topical Conference on the Structure of the $1f_{7/2}$ Nuclei,* edited by R. A. Ricci (see Ref. 12), p. 37.
[19]W. E. Dorenbusch, T. A. Belote, and J. Rapaport, Nucl. Phys. A109, 649 (1968).
[20]F. B. Malik and W. Scholz, Phys. Rev. 150, 919 (1966).
[21]O. Hausser, D. Pelte, T. K. Alexander, and H. C. Evans, Nucl. Phys. A150, 417 (1970).
[22]P. M. S. Lesser, D. Cline, P. Goode, and N. Horoshko, Nucl. Phys. A190, 597 (1972).
[23]N. V. DeCastro Faria, J. Charbonneau, J. L'ecuyer, and R. J. A. Levesque, Nucl. Phys. A174, 37 (1971).
[24]T. T. Bardin, J. A. Becker, and T. R. Fisher, Phys. Rev. C 7, 190 (1973).
[25]G. Fortune, Ph.D. thesis, University of Padova, Italy, 1973.